PHILOSOPHICAL TRANSACTIONS OF THE ROYAL SOCIETY A

Phil. Trans. R. Soc. A (2005) **363**, 1603–1623
doi:10.1098/rsta.2005.1597
Published online 1 July 2005

Rotational flow in gravity current heads

By J. N. McElwaine

Department of Applied Mathematics and Theoretical Physics, Centre for Mathematical Sciences, University of Cambridge, Wilberforce Road, Cambridge CB3 0WA, UK
(jnm11@damtp.cam.ac.uk)

The structure of gravity currents and plumes, in an unbounded ambient, on a slope of arbitrary angle is analysed. Inviscid, rotational flow solutions in a wedge are used to study the flow near the front of a current, and used to show that the Froude number is $\sqrt{2}$ and the angle of the front to the slope is 60°. This extends the result of von Kármán (1940) to arbitrary slope angles and large internal current velocities. The predictions of the theory are briefly compared with experiments and used to explain the large negative (relative to ambient) pressures involved in avalanches.

Keywords: gravity current; plume; wedge flow

1. Introduction

Gravity currents are flows driven by density differences and occur in many situations (Simpson 1997). Early analytic work of von Kármán (1940) assumed that inside the flow the pressure distribution was hydrostatic, and this assumption has been used in later work with integral models and shallow-water equations. By setting up a balance between the pressure of the irrotational ambient fluid flow along the front of a gravity current and the hydrostatic pressure in the gravity current von Kármán (1940) showed that the front makes an angle of 60° to the horizontal. Benjamin (1968) extended this work and calculated an approximate analytic expression for the shape of the front when the flow depth is half the depth of the ambient fluid; the only case without dissipation.

However, recent results from direct numerical simulations and experiments have shown that in some cases the pressure inside these flows is far from hydrostatic (see figure 1). In fact pressures well below ambient pressure can be observed indicating the presence of large internal velocities.

In this paper we use the term *gravity current* to refer to buoyancy driven flows on slopes of arbitrary angle, thus including vertical plumes as one extreme and horizontal gravity currents as the other. We show that for finite volume releases in an unbounded ambient the similarities are much stronger than has previously been realized. In particular we show that the angle of the front relative to the slope is 60° and that the Froude number is approximately $\sqrt{2}$ *for all slope angles.* The analysis solves the steady Euler equations near the intersection of the front

One contribution of 11 to a Theme 'Geophysical granular and particle-laden flows'.

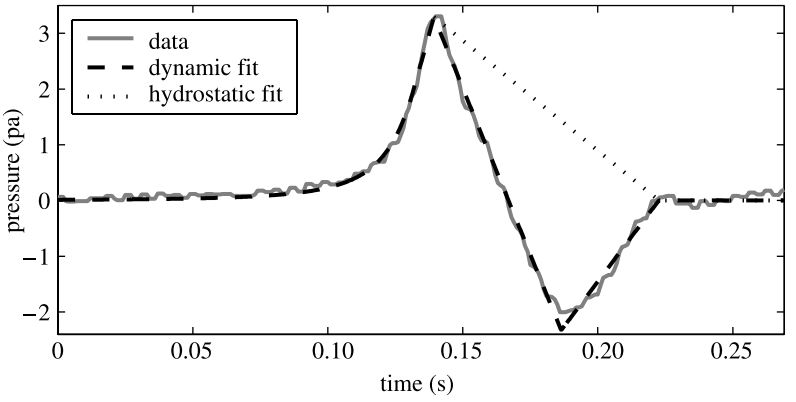

Figure 1. Air pressure at the base of a small powder snow avalanche compared with a fit to the theory presented in this paper (labelled dynamic fit) and the standard hydrostatic assumption (labelled hydrostatic fit).

surface with the slope in the current and in the ambient. The Reynolds number is assumed to be high enough that the viscosity can be neglected and the Euler equations hold. Questions of stability are not addressed and turbulence is ignored. We will assume that the current is denser than the ambient and thus runs on the upper surface of the slope, but the reverse case of a lighter current running up the underside of the slope is covered by the same analysis.

2. Flow in a wedge

Figure 2 shows a sketch of the flow in the vicinity of the front. We will work in r, θ polar coordinates centred at O, the intersection of the front with the slope, and denote the coordinate unit vectors by $\hat{\boldsymbol{r}}$ and $\hat{\boldsymbol{\theta}}$. Working to lowest order in r the front will be a straight line defined to be an angle $\Phi = 2\phi_2$ to the surface. We assume that the flows are continuous in both regions and that the normal velocity vanishes between the regions and on the surface, but that the tangential velocity does not have to be continuous across surfaces. That is, we are considering the high Reynolds number case where the boundary layers are small compared to the thickness of the gravity current. The pressure must be continuous everywhere.

The steady Euler equations (Navier–Stokes equation without viscosity for an incompressible fluid) are

$$\nabla \cdot \boldsymbol{u} = 0, \tag{2.1}$$

$$\boldsymbol{u} \cdot \nabla \boldsymbol{u} + \frac{1}{\rho} \nabla p = \boldsymbol{g}, \tag{2.2}$$

where $\boldsymbol{u}$ is the fluid velocity, ρ the density, p the pressure and $\boldsymbol{g}$ the acceleration due to gravity. Figure 2 shows that both the flow in the ambient and the current are flows in a wedge with half angles ϕ_1 and ϕ_2. Thus we proceed by finding the general solution of equations (2.1) and (2.2) for flow in a wedge of half angle ϕ. For a wedge with rigid walls the boundary condition is that the normal velocity

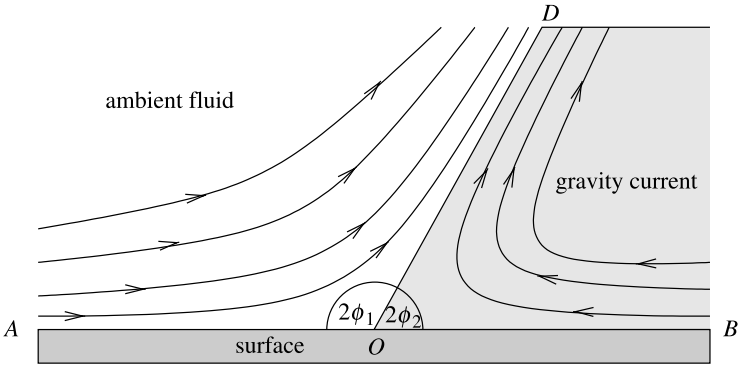

Figure 2. Schematic in the vicinity of the front $\phi_1+\phi_2=\pi/2$.

vanishes, that is $\hat{\boldsymbol{\theta}}\cdot\boldsymbol{u}|_{\theta=\pm\phi}=0$. If we define a stream function $\psi(r,\,\theta)$ by

$$\boldsymbol{u}=\frac{\hat{\boldsymbol{r}}}{r}\psi_\theta-\hat{\boldsymbol{\theta}}\psi_r, \tag{2.3}$$

where the subscripts denote differentiation, then the continuity equation (2.1) for incompressible fluids is automatically satisfied. The pressure can be eliminated by taking the curl of equation (2.2) to give the vorticity equation

$$\boldsymbol{u}\cdot\nabla\omega=0, \tag{2.4}$$

where

$$\omega=-\frac{\psi_{\theta\theta}}{r^2}-\frac{(r\psi_r)_r}{r}, \tag{2.5}$$

is the vorticity.

We consider a solution to lowest order in r. For the solution to be non-singular the lowest order term must contain a power of r, so we look for solutions of the form

$$\psi(r,\theta)=cr^\alpha f(\theta), \tag{2.6}$$

where c is a constant with units of $[L^{1-\alpha}T^{-1}]$ and $f(\theta)$ is dimensionless. Since the streamfunction must be bounded, it is convenient to choose c so that $f(\theta_{\max})=1$ for some $|\theta_{\max}|\leq\phi$. The anomalous dimension[1] of c lies in the limit $r/H\to0$, where H is the height of the current (defined in figure 3). With this choice

$$\boldsymbol{u}=\hat{\boldsymbol{r}}r^{\alpha-1}cf_\theta-\hat{\boldsymbol{\theta}}\alpha r^{\alpha-1}cf, \tag{2.7}$$

$$\omega=-cr^{\alpha-2}(f_{\theta\theta}+\alpha^2 f). \tag{2.8}$$

From equation 2.7 the boundary condition $\hat{\boldsymbol{\theta}}\cdot\boldsymbol{u}|_{\theta=\pm\phi}=0$ then gives two boundary conditions on $f(\theta)$

$$f(\pm\phi)=0. \tag{2.9}$$

[1] See Goldenfeld (1992) for a full explanation especially exercise 10-4.

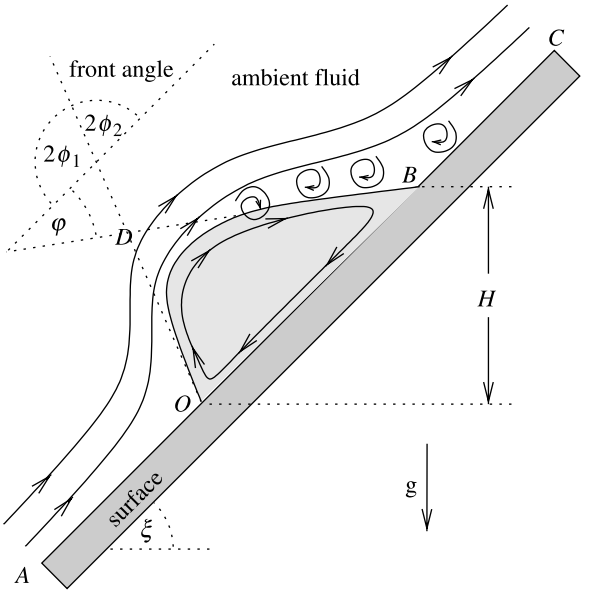

Figure 3. Schematic of a gravity current on an incline.

Substituting equations (2.7) and (2.8) into equation (2.4) gives

$$\alpha f f_{\theta\theta\theta} + (2-\alpha) f_\theta f_{\theta\theta} + 2\alpha^2 f f_\theta = 0. \tag{2.10}$$

There are two special cases. When $\alpha=0$ equation (2.10) becomes $f_{\theta\theta}=0$ which cannot satisfy simultaneously $f(\pm\phi)=0$ and $f(\theta_{\max})=1$. The case $\alpha=1$ is discussed in Appendix A(c). Henceforth we exclude these cases. Equation (2.10) can be integrated to give

$$\alpha f f_{\theta\theta} + (1-\alpha) f_\theta^2 + \alpha^2 f^2 + \alpha^2(\alpha-1)A = 0, \tag{2.11}$$

where A is a constant of integration. Equation (2.11) can be written

$$\frac{\alpha f^{3-2/\alpha+3}}{2f_\theta} \frac{\mathrm{d}}{\mathrm{d}\theta}\left[f^{2/\alpha-2}(f_\theta^2 + \alpha^2 f^2 - A\alpha^2)\right] = 0, \tag{2.12}$$

which can be integrated to give

$$1/\alpha^2 f_\theta^2 = A - f^2 + B f^{2-2/\alpha}, \tag{2.13}$$

where B is another constant of integration. Writing $h=f^{1/\alpha}$ equation (2.13) becomes

$$h_\theta^2 = a - h^2 + b h^{2-2\alpha}, \tag{2.14}$$

where a and b are two new constants. By definition the maximum value of f, and hence h, is one, and this must occur interior to the interval, since from equation (2.9) $f=h=0$ on the edges, thus when $h=1$, $h_\theta=0$, which implies $b+a=1$. Thus we can write

$$h_\theta = \pm\sqrt{1 - h^2 + b(h^{2-2\alpha} - 1)}, \tag{2.15}$$

Table 1. *Special case solutions to equation (2.16) including singular cases* $\alpha \leq 1$
(The derivations are contained in the appendix.)

α	ϕ	ψ	note
α	$\pi/2$	$(r\cos\theta)^\alpha$	shear
α	$\pi/(2\alpha)$	$\mathrm{r}^\alpha \cos(\alpha\theta)$	irrotational
α	$\phi \ll 1$	$1-\frac{\theta}{\phi} = I_{h^{2(\alpha-1)}}\left(\frac{\alpha}{2(\alpha-1)}, \frac{1}{2}\right) + O(\phi^2)$	small angle
$\ll -1$	ϕ	$r^\alpha\left(\frac{\sin(\phi-\theta)}{\sin\phi}\right) + O\left(\frac{1}{\sqrt{-\alpha}}\right)$	singular
$1/2$	ϕ	$\sqrt{r}\sqrt{1-\frac{\sin^2\frac{\theta}{2}}{\sin^2\frac{\phi}{2}}}$	singular
1	ϕ	$\approx r\frac{(1+b)\cos(\theta\sqrt{1-b})-2b}{1-b}$ [a]	
$3/2$	ϕ	see Appendix A (d)	linear pressure
2	ϕ	$r^2\left(1-\frac{\sin^2\theta}{\sin^2\phi}\right)$	
$\ll 1$	ϕ	$r^\alpha\cos\theta + O(1/\alpha)$	$\lvert\theta\rvert < \phi - O\left(\frac{1}{\alpha}\right)$

[a]For $\alpha=1$, b is defined implicitly by $(1+b)\cos\left(\phi\sqrt{1-b}\right) = 2b$.

with solution

$$\int_h^1 \frac{\mathrm{d}h}{\sqrt{1-h^2+b(h^{2-2\alpha}-1)}} = |\theta|. \tag{2.16}$$

There appears to be no general closed form expression for this integral. For $\alpha > 1$ this has real solutions on $h \in [0,1]$ for all positive b. The boundary condition, equation (2.9), gives an implicit equation for b as a function of ϕ and α

$$\int_0^1 \frac{\mathrm{d}h}{\sqrt{1-h^2+b(h^{2-2\alpha}-1)}} = \phi. \tag{2.17}$$

The integrand is a monotonic decreasing function of b for all $\alpha > 1$ and $h \in [0,1)$. Thus the integral is also decreasing from $\pi/2$ at $b=0$ and tends to 0 for large b. So there are solutions $b(\phi, \alpha)$ for all $\phi < \pi/2$ and $\alpha > 1$. Some exact and approximate solutions are shown in table 1, where singular solutions have been included for completeness.

Equation (2.15) can be used to rewrite equation (2.7) and (2.8)

$$\boldsymbol{u} = -c\alpha r^{\alpha-1}\left[\mathrm{sgn}(\theta)\hat{\boldsymbol{r}}\sqrt{(1-b)h^{2(\alpha-1)} - h^{2\alpha} + b} + \hat{\boldsymbol{\theta}}h^\alpha\right], \tag{2.18}$$

$$\omega = c\alpha(1-b)(1-\alpha)(rh)^{\alpha-2}. \tag{2.19}$$

Equation (2.19) shows that non-trivial ($c \neq 0$) and non-singular ($\alpha > 1$) solutions are irrotational if and only if $b=1$ and in this case $\phi = \pi/(2\alpha)$. On the slope and front surface $h(\pm\phi) = 0$, so the vorticity is infinite if $\alpha < 2$, constant if $\alpha = 2$ and zero if $\alpha > 2$. The velocity on the boundary can also be calculated by substituting

$h=0$ into equation (2.18) to give

$$\boldsymbol{u}(\pm\phi) = \mp c\alpha\sqrt{b}r^{\alpha-1}\hat{\boldsymbol{r}}. \tag{2.20}$$

Thus the velocity is known on the boundary without having to solve explicitly for h.

Equation (2.15) can now be used to solve for the pressure field $p(r,\ \theta)$. Substituting equations (2.3) and (2.6) into equation(2.2) it becomes

$$-\rho c^2\alpha^2 r^{2\alpha-3}h^{2\alpha-1}(h_{\theta\theta}+h)\hat{\boldsymbol{r}} + p_r\hat{\boldsymbol{r}} + p_\theta/r\hat{\theta} = \rho\boldsymbol{g}. \tag{2.21}$$

Eliminating the derivative of h with equation (2.15) we get

$$\rho bc^2\alpha^2(\alpha-1)r^{2\alpha-3}\hat{\boldsymbol{r}} + p_r\hat{\boldsymbol{r}} + p_\theta/r\hat{\boldsymbol{\theta}} = \rho\boldsymbol{g}, \tag{2.22}$$

which has solution

$$p = \rho r\hat{\boldsymbol{r}}\cdot\boldsymbol{g} - \tfrac{1}{2}\rho bc^2\alpha^2 r^{2\alpha-2}. \tag{2.23}$$

The pressure is only defined up to an arbitrary constant and in this section we take $p=0$ at the origin. This solution is most easily verified by substitution and has the surprising result that the only dependence on angle is through gravity. It is non-singular for all $\alpha>1$.

3. Matching

(*a*) *Front of the flow*

These wedge solutions are valid in an intermediate zone. Near the bottom surface there will be a viscous boundary layer satisfying a no-slip condition, and on the boundary between the fluids (AD) there must also be a boundary layer. We neglect these regions and simply match the pressure across the fluid interface. This is valid because the pressure will not change significantly across a boundary layer. We consider matching general wedge flows, but in the case of a gravity current the incoming ambient fluid must be irrotational since there is no source of vorticity. However, inside the gravity current vorticity can be generated in the head, at the basal surface and on the front and then advected back into the flow and cannot be determined by our analysis. We label α_i, where $i=1$ for the ambient and $i=2$ for the gravity current, and similarly for ϕ_i, b_i and c_i.

From equation (2.23) the pressure in each fluid along their boundary OD (see figure 3) is

$$p_i(r) = -\rho_i r g' - \tfrac{1}{2}\rho_i b_i c_i^2 r^{2(\alpha_i-1)}, \tag{3.1}$$

where $g'=g\sin(\xi+2\phi_1)$ is the component of gravity along the boundary and the only term that depends on the slope angle ξ (see figure 3). Therefore equating the pressures across the front, $p_1(r)=p_2(r)$, gives

$$2(\rho_2-\rho_1)g'r + \rho_2 b_2 c_2^2 r^{2(\alpha_2-1)} - \rho_1 b_1 c_1^2 r^{2(\alpha_1-1)} = 0. \tag{3.2}$$

The three terms of this equation can be in balance, to lowest order in r, in different ways. If all three terms are identically zero this corresponds to fluids of identical density at rest and any front angle is possible.

If the fluids have identical density but are not both at rest then the flow corresponds to a stationary separation point. Equation (3.2) becomes

$$b_2 c_2^2 r^{2(\alpha_2-1)} = b_1 c_1^2 r^{2(\alpha_1-1)}. \tag{3.3}$$

Thus $\alpha_1=\alpha_2$ and $b_1c_1^2=b_2c_2^2$, so both fluids must be in motion. The velocity across the front is continuous if c_1 and c_2 have the same sign. Any angle is possible if at least one of the flows is irrotational. If both flows are irrotational then $\phi_1=\phi_2=\pi/(2\alpha)$ and since $\phi_1+\phi_2=\pi/2$ we must have $\phi_1=\phi_2=\pi/4$, that is, the front is perpendicular to the slope surface.

If $\rho_2\neq\rho_1$, we take without loss of generality that $\rho_2>\rho_1$ and $g'>0$. Since the $b_i\geq1$ the second term in equation (3.2) is positive and cannot balance the first term. Thus there are three possibilities, the first and the third term balance, the second and third terms balance, or all three terms balance (to lowest order in r).

If the first and third terms balance then $\alpha_1=3/2$ and $\alpha_2>3/2$ and equation (3.2) is

$$2(\rho_2-\rho_1)g' = \rho_1 b_1 c_1^2 + o(r). \tag{3.4}$$

This is the same as neglecting the dynamic pressure in the current. If the flow in the ambient fluid is rotational then any angle ϕ_1 is possible and this will be determined by the vorticity of the ambient fluid in the vicinity of the stagnation point. If however the flow is irrotational then thus $\phi_1=\pi/(2\alpha_i)=\pi/3$ so the front angle $\Phi=\pi-2\phi_1=\pi/3=60^\circ$.

If the second and third terms balance then $\alpha_1=\alpha_2<3/2$, This is similar to the case where the fluids have identical density, but the velocity will be discontinuous across the front. When the ambient fluid is irrotational however the following argument excludes this possibility. From equation (2.5), when $\omega=0$, the stream function satisfies the *linear* equation

$$\psi_{\theta\theta} + r(r\psi_r)_r = 0, \tag{3.5}$$

with boundary conditions $\psi(r,\ \pm\phi_1)=0$. The general, non-singular solution of equation (3.5) is

$$\psi = \sum_{n=0}^{\infty} e_n r^{(n+1/2)\pi/\phi_1}\cos[(n+1/2)\pi\theta/\phi_1], \tag{3.6}$$

where e_n are constants. Bernoulli's theorem along the streamline OD ($\theta=-\phi_1$) gives the pressure

$$p_1(r,-\phi_1) = -\tfrac{1}{2}\rho_1 \sum_{m,n=0}^{\infty} e_n e_m (-1)^{n+m} r^{(n+m+1)\pi/\phi_1-2}. \tag{3.7}$$

If one of these terms balances the linear hydrostatic contribution then $(n+m+1)\pi/\phi_1-2=1$ for some non-negative integers n and m so $\phi_1=(n+m+1)\pi/3$ and the front angle $\Phi=\pi-2\phi_1=\pi(1-2n-2m)/3$. Thus the only positive front angle is $\pi/3=60^\circ$ when $n=m=0$.

The other possibility is that a pressure term in the current is linear in r and balances the hydrostatic term. Suppose that the leading order term in the stream function in the current, has power α and there is another term with power α' so that

$$\psi = cr^{\alpha} f(\theta) + c' r^{\alpha'} f'(\theta) + \ldots, \tag{3.8}$$

where c' is a constant and f and f' undetermined functions of θ. Bernoulli's theorem along the streamline OD ($\theta = \phi_2$) shows that the dynamic contribution to the pressure is

$$-\tfrac{1}{2}\rho_2[c^2 r^{2\alpha-2} f^2 + c' 2 r^{2\alpha'-1} f' 2 + 2cc' r^{\alpha+\alpha'-2} f f' + \ldots]. \tag{3.9}$$

The first two terms are non-negative, so the only term that can be negative and balance the hydrostatic term is the cross term $2cc' r^{\alpha\alpha'-2} f f'$ if $\alpha + \alpha' - 2 = 1$ and $cc' f f' < 0$. The other two terms must balance with terms from equation (3.7) so that $\pi/\phi_1 = 2\alpha$ and $(n+1)\pi/\phi_1 = 2\alpha'$. Eliminating α and α' from these three equations we get $\phi_1 = (n+2)\pi/6$ giving front angles $\Phi = \pi(1-n)/3$. Thus again the only positive front angle possible is $\pi/3 = 60°$.

This argument assumes that the front is straight to second order and can only be made rigorous, by a full second order analysis. This result also proves that solutions such as Hill's spherical vortex, or its two-dimensional equivalent, cannot be in balance for different densities since $\alpha = 2$. In fact apart from degenerate cases the stagnation point must be non-analytic.

The last case to consider is when all three terms are in balance so that $\alpha_1 = \alpha_2 = 3/2$. Then if the ambient fluid is irrotational $\phi_1 = \pi/3$ and $\phi_2 = \pi/6$, so that the front angle is 60°.

This argument has shown that the leading order term in the irrotational ambient fluid stream function must be $r^{3/2}$ and there can be no lower order term in the current. The results of the previous section for wedge flows then show that this means that the front angle must be 60° thus generalizing the result of von Kármán (1940) to currents on slopes of any angle with significant internal motions. Note that the front angle is relative to the slope and holds even when the slope is inclined, so that the front may be beyond vertical and this is observed in experiments (see figure 4).

(*b*) *Rear of the flow*

Similar analysis can also be performed at the rear of the flow, but there are several differences. In general the ambient flow will separate and mix as it passes over the gravity current head and B will be in a turbulent wake. Whether there is a clear interface between the current and the ambient, so that point B is well defined, will depend on the slope angle and the nature of the two fluids. If the two fluids can mix then the rear boundary will be ill-defined even on shallow slopes. If the current is a particulate suspension or an immiscible fluid then the rear boundary may reform at the tail of the flow even if there is substantial mixing in the vicinity of the head. We consider this case where there is a clear boundary at the tail of the flow in the vicinity of B and we assume that the mean pressure in the wake is 0.

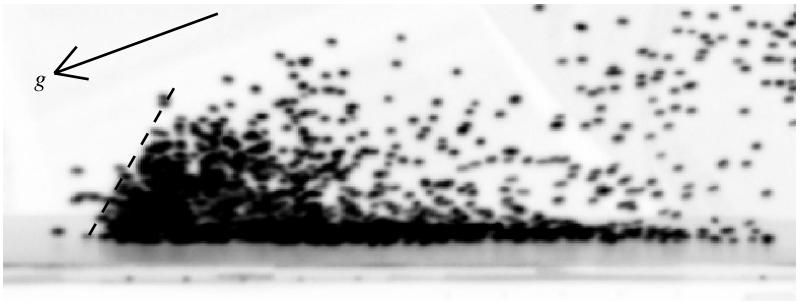

Figure 4. Polystyrene ball gravity current on 70° surface. The dotted line is drawn at 60° to the surface and is approximately parallel to the front. The solid black line labelled $\boldsymbol{g}$ is vertical. The colours are reversed. Saltating balls in the turbulent tail can be seen. Once the head has formed the angle is roughly constant down the slope and does not depend on the number of balls or the slope angle (J. N. McElwaine, unpublished work).

The flow of the current in the vicinity of B will also be a wedge flow, so matching the zero mean pressure in the ambient with the pressure in the current, similarly to equation (3.2) gives

$$2(\rho_2 - \rho_1)rg\sin(\varphi - \xi) + \rho_2 b_3 c_3^2 r^{2(\alpha_3 - 1)}, \tag{3.10}$$

where r is a radial coordinate measured from B and b_3, c_3 and α_3 are wedge flow solution coefficients. The solution of this is $\varphi \leq \xi$, $\alpha_3 = 3/2$ and $2(\rho_2 - \rho_1)g\sin(\xi - \varphi) = \rho_2 b_3 c_3^2$. A special case of this corresponds to a horizontal, hydrostatic tail with $\varphi = \xi$ and $c_3 = 0$ and is expected on shallow inclines. The crucial difference with equation (3.2) is that the hydrostatic term is negative if $\varphi < \xi$ and can be balanced by flow in the current. Since the flow need not be rotational the angle φ is not specified.

(*c*) *Flow reflection*

A feature of these wedge flows is that the streamlines are symmetric and in particular $\boldsymbol{u}(\phi) + \boldsymbol{u}(-\phi) = \boldsymbol{0}$. When the flows have this symmetry in the ambient and in the current there is a general relation between the pressure along the surface in front of the current (p_{OA}) and the pressure along the surface inside the current (p_{OB}) that only depends on the slope and front angles, fluid densities and gravity. Let $u_i^2(r) = \boldsymbol{u}_i^2(r, \pm\phi_i)$ then

$$\left.\begin{aligned} p_{OA}(r) &= p_1(r, \phi_1) = -\tfrac{1}{2}\rho_1 u_1^2 - g\rho_1 r\sin(\xi + \pi) \\ p_{OC}(r) &= p_1(r, -\phi_1) = -\tfrac{1}{2}\rho_1 u_1^2 - g\rho_1 r\sin(\xi + \Phi) \\ &= p_2(r, \phi_2) = -\tfrac{1}{2}\rho_2 u_2^2 - g\rho_2 r\sin(\xi + \Phi) \\ p_{OB}(r) &= p_2(r, -\phi_2) = -\tfrac{1}{2}\rho_2 u_2^2 - g\rho_2 r\sin(\xi). \end{aligned}\right\} \tag{3.11}$$

Eliminating u_1 and u_2 from these equations we get

$$p_{OB} = p_{OA} - 2g\rho_1 r\sin\xi + g(\rho_2 - \rho_1)r[\sin(\xi + \Phi) - \sin\xi]. \tag{3.12}$$

The second term in this equation is the background hydrostatic pressure of the ambient fluid. The third term can be positive, zero or negative depending on $\xi+\Phi/2<\pi/2$, $\xi+\Phi/2=\pi/2$ or $\xi+\Phi/2>\pi/2$ respectively. Since $\Phi=\pi/3=60^\circ$ the angle at which the sign changes is $\xi=\pi/2-\Phi/2=\pi/3=60^\circ$ as one would expect on symmetry grounds. For other slope angles, equation (3.12) can be used to infer the density of the flow when it is unknown according to

$$\rho_2/\rho_1 = 1 + \frac{(p_{OB} - p_{OA})/(g\rho_1 r) + 2\sin\xi}{\sin(\xi+\Phi) - \sin\xi}, \tag{3.13}$$

which is similar to the difference in the pressure gradients. Any deviations from the prediction of equation (3.12) are indications of asymmetry in the flow fields.

The same argument can be used in the vicinity of the rear stagnation point B to show

$$p_{BO} = p_{BD} + g\rho_2 r[\sin\xi - \sin(\xi-\varphi)], \tag{3.14}$$

$$= p_{BC} + 2g\rho_1 r\sin\xi + g(\rho_2-\rho_1)r[\sin\xi - \sin(\xi-\varphi)], \tag{3.15}$$

where r measures distance from B.

(*d*) *Continuity*

Equation (3.2) shows that it is impossible to simultaneously match the tangential velocity and the pressure across the front, thus there must be a boundary layer, where viscosity is important and vorticity is generated. From equation (2.20), the velocity difference across the front is

$$\Delta u = \tfrac{3}{2}\sqrt{r}[\sqrt{b_1}c_1 + \sqrt{b_2}c_2]. \tag{3.16}$$

Substituting for $\sqrt{b_1}c_1$ from equation (3.2) and w.l.g $c_1<0$ and $c_2>0$ this becomes

$$\Delta u = \tfrac{3}{2}\sqrt{r}\left[\sqrt{b_2}c_2 - \sqrt{2\left(\frac{\rho_2}{\rho_1}-1\right)g' + \frac{\rho_2}{\rho_1}b_2c_2^2}\right]. \tag{3.17}$$

This is always negative for $g'>0$ and $\rho_2>\rho_1$.

4. Global flow

Figure 3 shows a schematic of the whole flow. Our analysis has taken place in the vicinity of the origin O and is valid over distances for which the front is straight, that is distances small compared to its radius of curvature. The question then is how to couple this local flow pattern to the global flow. The flow of the ambient fluid far in front of the current is straightforward and was analysed in McElwaine & Nishimura (2001). However, to couple this far field solution to the flow in the vicinity of the front and inside is not straightforward. Some useful results however can be shown without tackling this, by considering a line on the surface passing through $AOBC$. On this line the fluid velocity perpendicular to the surface must be zero, so, though it is not a streamline, Bernoulli's theorem applies. We continue to assume that the gravity current is in approximate dynamic equilibrium, so that

the rest frame of the current is not accelerating and the velocity of the ambient fluid tends to U (parallel to the surface) at infinity. Henceforth, we consider a pressure field in which the hydrostatic pressure due to the ambient has been subtracted off and we take the pressure at infinity to be 0. In front of the flow at distances r large compared to H the flow field is well approximated by a dipole (McElwaine & Nishimura 2001) so the pressure on the surface between A and O is

$$p_d(r) = \tfrac{1}{2}\rho_1 U^2 \frac{R^3}{(r+r_0)^3}\left(2 - \frac{R^3}{(r+r_0)^3}\right), \tag{4.1}$$

where r_0 is a coordinate offset and R is the effective aerodynamic radius of the current. r_0 is the offset off O from the effective centre of the current. We will make the natural choice $r_0 = R$ which corresponds to setting the point O to be on the surface of the effective sphere.

As we approach O the solution must change to

$$p_1(r) = \tfrac{1}{2}\rho_1 U^2\left(1 - \kappa\frac{r}{R}\right), \tag{4.2}$$

where $\kappa = Rc_1^2 b_1/U^2$ is a non-dimensional constant. This satisfies Bernoulli's theorem as the pressure is $(1/2)\rho_1 U^2$ for $r=0$. We blend the two solutions together by requiring that the pressure and its first derivative are continuous everywhere[2] between A and O, in particular at the point $r=(\lambda-1)R$ where we switch between the two solutions. This results in the following two equations

$$1 - \kappa\lambda = \frac{1}{\lambda^3}\left(2 - \frac{1}{\lambda^3}\right), \tag{4.3}$$

$$-\kappa = 6\frac{1-\lambda^3}{\lambda^7}. \tag{4.4}$$

These have solution $\lambda = (1/6)(676 + 36\sqrt{353})^{1/3} - (4/3)(676 + 36\sqrt{353})^{-1/3} - (1/3) \approx 1.39$ with κ then given by equation 4.4 so $\kappa \approx 1.01$. With these choices there is no practical difference between the blended solution and the purely dipole solution since the dipole solution is almost linear for small r (maximum relative error is less than 5%).

Crossing the flow front at O the pressure must still be continuous, but its derivative need not, because there will be a thin boundary layer where viscous effects are important. From equations (3.12) and (4.2) the pressure inside the gravity current on the slope surface is

$$p_2(r) = \tfrac{1}{2}\rho_1 U^2\left(1 - \kappa\frac{r}{R}\right) + 2g(\rho_2 - \rho_1)r\sin(\phi_2)\cos(\xi + \phi_2). \tag{4.5}$$

This should be valid over a similar range of small r/R to equation (4.2). The hydrostatic contribution from the ambient fluid has been dropped from equation (3.12). Equation (3.12) cannot be used for larger r/R since the front will not be straight.

Moving further away from O towards B the speed and pressure are unknown but Bernoulli's theorem must hold. Thus $(1/2)\rho_1 U^2 = (1/2)\rho_2 u_x^2 +$

[2] This must be the case for an irrotational solution of the Euler equations to be valid.

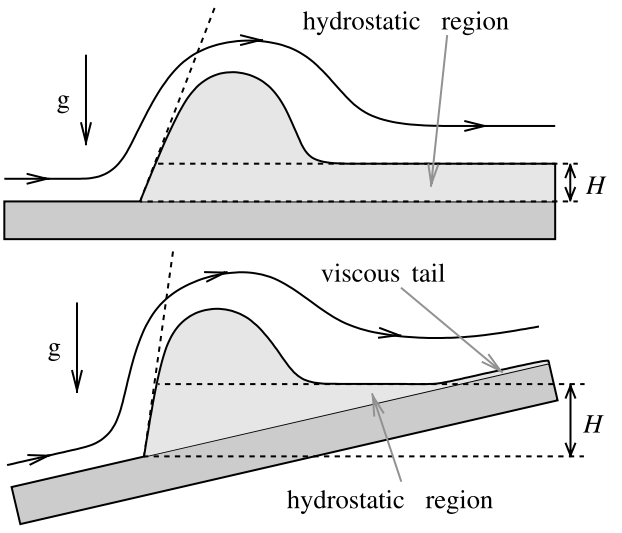

Figure 5. Schematics of gravity currents on a flat surface and a low incline slope, with a viscous tail.

$p + g(\rho_2 - \rho_1)r\sin\xi$, where u_x is the (unknown) velocity parallel to the surface. Since the flow is stationary the velocity at B must be zero, therefore $p_B = (1/2)\rho_1 U^2 - g(\rho_2 - \rho_1)H$, where H is shown in figures 3 and 5 and is defined to be the vertical distance between the front of the current and the tail ignoring any viscous region. Behind the current the flow separates and is turbulent, so that dissipation of energy and other viscous effects are important. That is the fluid between B and C is accelerated back to U by viscous forces and there is no pressure drop so that $p_B = p_C = 0$. Therefore

$$\tfrac{1}{2}\rho_1 U^2 = g(\rho_2 - \rho_1)H \Rightarrow \mathrm{Fr} = \sqrt{2}, \tag{4.6}$$

where $\mathrm{Fr} = U/\sqrt{g(\rho_2/\rho_1 - 1)H}$ is the densimetric Froude number. This recovers the standard result of von Kármán (1940) (with a corrected argument by Benjamin 1968), but for an inclined surface. In the case when the surface is flat the result still holds, but with an extra assumption that far from the front the pressure inside the gravity current is hydrostatic and not just on the surface.

Putting these results together we now have a theory for the pressure all along the surface except in the latter part of the current.

$$p = \begin{cases} \tfrac{1}{2}\rho_1 U^2 \dfrac{R^3}{(r+R)^3}\left(2 - \dfrac{R^3}{(r+R)^3}\right) & OA \quad r/R > \lambda - 1 \\ \tfrac{1}{2}\rho_1 U^2\left(1 - \kappa\dfrac{r}{R}\right) & OA \quad r/R < \lambda - 1 \\ \tfrac{1}{2}\rho_1 U^2\left(1 - \kappa\dfrac{r}{R}\right) + 2g(\rho_2 - \rho_1)r\sin(\phi_2)\cos(\xi + \phi_2) & OB \quad r/R < O(\lambda - 1) \\ \text{unknown} & OB \quad r/R = O(\lambda - 1) \\ \approx 0, \text{ but turbulent fluctuations} & BC. \end{cases} \tag{4.7}$$

It does not seem likely that there can be any simple, general theory that covers the latter part of the current (marked as unknown in equation 4.7) for all slope angles since in general the flow will be turbulent with many eddies. The wake of the current may also be turbulent, and the pressure may fluctuate significantly about zero. In some cases however equations (3.10) and (3.14) might be applicable. In the §5 we give a comparison of this theory with one experiment.

This section has given a very rough approach for matching the near field solution to the far field solution, requiring that the pressure and its first derivative are continuous along the line AOB. However there is no continuous transition between the two solutions accept on this line. A curve separating the plane into regions for the two solutions, so that the total solution is continuous, can be found for certain choices of parameters. However, the derivative of the pressure along AOB is then discontinuous and poorly matches the data. A more sophisticated approach needs to make an expansion in the vicinity of the front that includes two length scales related to the width and the height of the flow.

5. Discussion

(*a*) *Implications*

One prediction that can be made from these results on front angle and Froude number is the dependence of flow speed on flow volume. Figure 6 shows three idealized flow profiles corresponding to different models. In case (i) the flow front is assumed to be at 90° to the slope ($\Phi=\pi/2$) and corresponds to the shallow water approximation in coordinates parallel to the slope (Bonnecaze & Lister 1999). In case (ii) the flow front is assumed to be vertical (Webber *et al.* 1993) ($\Phi+\xi=\pi/2$) and corresponds to the shallow water equations in coordinates aligned with gravity. In both (i) and (ii) the flow is assumed to be hydrostatic so that the top surface is horizontal ($\phi=\xi$). In case (iii) the front angle is 60° ($\Phi=\pi/3$) to the slope and the top surface is below horizontal ($\phi<\xi$). This corresponds most closely to figure 4 where $\varphi\approx 20°$ and $\xi\approx 70°$. Assuming the flow has volume V and width W then simple trigonometry gives

$$V=\tfrac{1}{2}WH^2\frac{\sin\Phi\sin\varphi}{\sin^2\xi\sin(\Phi+\varphi)}. \tag{5.1}$$

For flat slopes ($\xi=0$) this relationship is singular as there are no finite volume, steady releases possible. Instead a finite flux gives rise to a steady current with finite H. In cases (i) and (ii) this relation is also singular as the slope angle becomes vertical ($\xi=\pi/2$). Case (iii) with $\Phi=\pi/3$, which we argue is the best approximation, does not suffer from this weakness. Combining equation (5.1) with the Froude number relation in equation (4.6) gives

$$U=\left[2g\left(\frac{\rho_2}{\rho_1}-1\right)\right]^{1/2}\left[\frac{2V}{W}\frac{\sin^2\xi\sin(\Phi+\varphi)}{\sin\Phi\sin\varphi}\right]^{1/4}. \tag{5.2}$$

This formula with $\Phi=\pi/3$ predicts the steady flow velocity for all slope angles between horizontal and vertical. With $\Phi+\xi=\pi/2$ and $\phi=\xi$ it reproduces

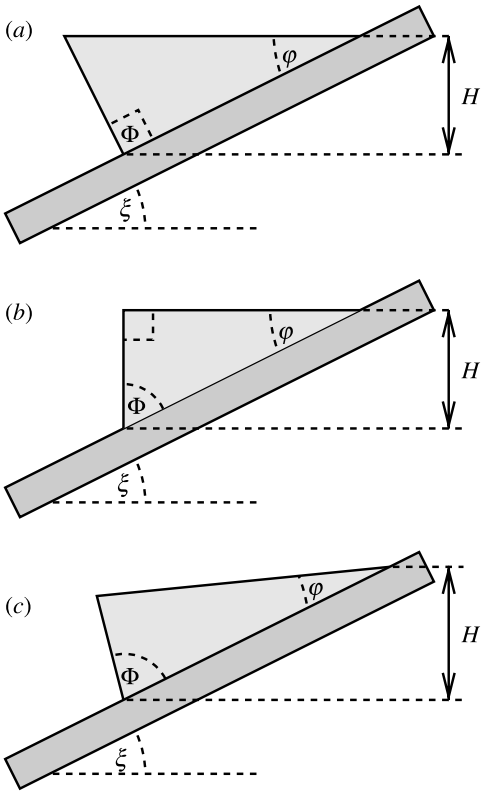

Figure 6. Schematics of gravity currents on slopes with different font and rear angles.

the result of Webber *et al.* (1993) where the flow depends on $\tan^{1/4}\xi$ which diverges for steep slopes. This calculation has assumed that the current has a triangular shape which is clearly not the case. However the tangent angles are correct at either end and one can hope that deviations from equations (5.1) and (5.2) can be accounted for by non-dimensional shape factors that are independent of slope angle. However, the rear angle of the current φ is unknown. On shallow slopes where there is a hydrostatic region at the rear it is equal to the slope angle ξ, but on steeper slopes the fluid in the current is accelerated on the upper surface by the ambient and any angle less than or equal to the slope angle is possible.

(*b*) *Comparison with experiment*

To illustrate the theory in this paper it is briefly compared with one experiment in a series (J. N. McElwaine & B. Turnbull, unpublished work). The experiment was carried out at the Swiss Federal Institute for Snow and Avalanche Research in Davos on an open chute of 3 m in length and angle $\xi = 70°$. The air pressure was measured 2.5 m down the centre of the slope through a small hole in the surface. Since the pressure is measured at a fixed point with a differential transducer the background hydrostatic contribution

from the ambient fluid can be ignored. Video observations confirmed that the flow was in dynamic equilibrium so its speed was roughly constant. In the rest frame of the current the sensor is then measuring the pressure at the point $r = U|t - t_0|$, where t_0 is the arrival time of the front at the sensor and U the speed of the current.

The parameters to be fitted are R and U from equation (4.7) the arrival time $t_0 \approx 0.14$ s, the pressure minimum and the time at which it occurs $t_1 \approx 0.19$ s, and the time at which the pressure returns to zero $t_2 \approx 0.22$ s. These were found using a least squares fitting procedure and the excellent agreement is shown in figure 1. The implied density ρ_2 can then be found using equation (4.7). The fitted pressure distribution gave the speed $U = 2.6\ \mathrm{m\ s^{-1}}$, the aerodynamic flow radius $R = 0.05$ m and the density of the flow $\rho_2 = 13\ \mathrm{kg\ m^{-3}}$. The speed and size are in agreement with the video observations. The density suggests a volume fraction of around 2% which is reasonable, but there was no independent measurement of this. The other curve in figure 1 shows a fit to a hydrostatic model where the internal velocities are zero so the pressure decreases linearly between t_0 and t_2, which is assumed to correspond to the end of the avalanche. This model suggests the internal density is $2.7\ \mathrm{kg\ m^{-3}}$. The total disagreement with a hydrostatic model is striking. It is remarkable that the pressure decrease inside the current is linear over a time of around 0.05 s corresponding to a distance of 0.13 m which is more than twice R, whereas in front of the flow the distance is approximately 0.8 R. This asymmetry, in contradiction to equation (3.12), shows that the front is not flat over such large distances and the flow is not wedge-like. This is presumably the result of a large eddy the centre of which corresponds to the pressure minimum at t_1. The linear fit between t_1 and t_2 is presumably the second half of the eddy. Note that this is in disagreement with equations (3.10) and (3.14–3.15). These predict that the pressure should decrease linearly as t increases towards t_2, whereas it is *increasing* linearly. This is probably because the rear edge is not well defined and the assumptions leading to these equations are therefore invalid. This may also be related to why the two estimates for the internal density are so different. The first estimate comes from the jump in the pressure gradient at t_0 and estimates the density at the front of the head. The second estimate comes from the total pressure drop across the current divided by its length so it measure the mean density. The large difference suggests that the density varies strongly in the current and is largest in the front, which is consistent with figure 4.

The sensor measures only the air pressure and does not measure any contribution from particle–particle contacts, either collisional or continuous. This distinction does not exist for fluid–fluid systems and is not important for low volume fraction suspension currents, where nearly all the stress is borne by the fluid. At higher particle concentrations where there maybe significant particle stresses, the measured air pressure will be lower and it would also be interesting to measure the particle stress on the surface. Though the measurements differ in this case the analysis is the same provided that the stress tensors for both the interstitial fluid and particles are isotropic—that is the stress tensor is pI were p is the pressure and I the identity matrix. This is a reasonable approximation provided that densities are sufficiently low so that there are few continuous contacts.

(c) *Extension to three-dimensional flows*

Over distances small compared to the radius of curvature of the front in the plane of the slope the conclusions of this paper are not effected. Extending the analysis to include three-dimensional spreading is rather difficult as the solution now needs to contain a line (intersection of the front with the slope) of non-analyticity. The only solution we have been able to find concerns a different case that is axisymmetric, so that there is only a single point of non-analyticity. In spherical polar coordinates the potential flow solution in the ambient fluid with linear pressure decrease is

$$\psi = r^{3/2} P_{3/2}(\cos\theta), \tag{5.3}$$

where P_γ is a Legendre function of order γ. The velocity field is

$$\boldsymbol{u} = \nabla\psi = \tfrac{3}{2}\sqrt{r} P_{3/2}(\cos\theta)\hat{\boldsymbol{r}} + \frac{3}{2}\frac{\sqrt{r}}{\sin\theta}\left[P_{3/2}(\cos\theta)\cos\theta - P_{1/2}(\cos\theta)\right]\hat{\boldsymbol{\theta}}, \tag{5.4}$$

where for this section only $\hat{\boldsymbol{r}}$ and $\hat{\theta}$ are unit vectors in spherical polar coordinates. The condition of zero normal velocity on a cone of half-angle ϕ is then

$$0 = \boldsymbol{u}\cdot\hat{\boldsymbol{\theta}}|_{\theta=\phi} = \frac{3}{2}\frac{\sqrt{r}}{\sin\phi}\left[P_{3/2}(\cos\phi)\cos\phi - P_{1/2}(\cos\phi)\right], \tag{5.5}$$

which has numerical solution $\phi \approx 115°$, corresponding to a front angle of 65°. Since there is no dependence on the azimuthal angle the pressure will only balance a flow falling down a vertical slope. Whether such half-cones flows with an angle of 65° exist would be an interesting experiment.

6. Conclusions

This paper has shown that the principal analytic results concerning gravity currents, namely $\Phi = 60°$ and Froude number is $\sqrt{2}$, are still valid for gravity currents on any slope from horizontal to vertical with or without significant internal velocities. At first sight these are a very surprising results, however, careful thought makes them obvious. The excess pressure due to the buoyancy in the flow must decrease linearly along the front, and the only irrotational flow with this property has an angle of 120° so the front angle must be 60°. The slope angle is irrelevant. The Froude number must be $\sqrt{2}$ (with suitably defined H) whenever it is reasonable to neglect dissipation and thus apply Bernoulli's law along a straight line close to the surface. It is also necessary that the pressure in the ambient fluid behind the head, where the depth H is defined, is approximately hydrostatic. That such a Froude number condition is satisfied even with significant vertical velocities at the front of a flow may help to explain the unreasonable effectiveness of the shallow water equations in describing such flows.

This theory provides an explanation for the large negative pressures that have been observed inside some gravity currents and the roughly constant front angle. Predictions are made concerning the velocity inside the gravity current which could be tested with direct numerical simulations (DNS). Further work is

necessary to match these solutions to the surface and across the front with boundary layers and to the ate the rear of the current.

The author is funded by the Isaac Newton Trust and the EU SATSIE project. The data shown in figure 1 was obtained with the help of Barbara Turnbull and Perry Bartelt at the Swiss Federal Institute for Avalanche Research (SLF) during a visit by the author funded by the Swiss National Science Foundation. The author would like to thank an anonymous referee for numerous comments and questions that have hopefully resulted in a more understandable paper.

Appendix A. Special cases

(*a*) $\alpha \ll -1$

The integrand in equation (2.16) can be approximated by writing

$$\frac{1}{\sqrt{1-h^2+b(h^\beta-1)}} = \frac{1}{\sqrt{1-h^2-b}\sqrt{1-\frac{-bh^\beta}{1-b-h^2}}}, \tag{A 1}$$

$$= \frac{1}{(1-h^2-b)^{1/2}} + \frac{-bh^\beta}{(1-h^2-b)^{3/2}} + O(h^{2\beta}), \tag{A 2}$$

where $\beta = 2-2\alpha$. The expansion is uniformly convergent and can be integrated since $(-bh^\beta/1-b-h^2) \leq 1$ for all $h \in [0,1]$ and $b<0$, thus it lies within the radius of convergence. The indefinite integral of the first term is $\sin^{-1} h/\sqrt{1-b}$. The second term of the series can be integrated asymptotically using Watson's lemma as $(2\sqrt{-b}\beta)^{-1} + O(\beta^{-2})$. Therefore

$$\sin^{-1} 1/\sqrt{1-b} - \sin^{-1} h/\sqrt{1-b} + O(1/\beta) = |\theta|. \tag{A 3}$$

Thus $b = -\cot\phi^2 + O(1/\beta)$ and

$$h = \frac{\sin(\phi-\theta)}{\sin\phi} + O(1/\sqrt{-\alpha}). \tag{A 4}$$

(*b*) $\alpha \gg 1$

Let $\beta = 2\alpha - 2$ and $b = g^\beta$. Then the integrand (2.16) is

$$\frac{1}{\sqrt{1-h^2+(g/h)^\beta - g^\beta}} \approx \begin{cases} 0 & h < g, \\ \dfrac{1}{\sqrt{1-h^2}} & h > g. \end{cases} \tag{A 5}$$

This can be made precise by splitting the integration into three part $[0,\ g(1-\delta/\beta)]$, $[g(1-\delta/\beta,\ g(1+\delta/\beta]$ and $[g(1+\delta/\beta,1]$. Over the first range let $h=g(1-\delta/\beta)x^{1/\beta}$ then

$$I_1 = \int_0^1 g\mathrm{d}x\left[\frac{1}{\beta\sqrt{x}\sqrt{(1-g^2)x^2+e^{\delta}}} + O\left(\frac{1}{\beta^2}\right)\right], \tag{A 6}$$

$$= \frac{2g\,\sin\,h^{-1}\left(\sqrt{1-g^2}e^{-\delta/2}\right)}{\beta\sqrt{1-g^2}} + O\left(\frac{1}{\beta^2}\right). \tag{A 7}$$

Over the second range let $h=g(1-x\,\delta/\beta)$ then

$$\left.\begin{aligned} I_2 &= \int_{-1}^1 g\delta\,\mathrm{d}x\left[\frac{1}{\beta\sqrt{1-g^2+e^{-\delta x}}} + O\left(\frac{1}{\beta^2}\right)\right] \\ &= \frac{2g}{\beta\sqrt{1-g^2}}\left[\sin\,h^{-1}\left(\sqrt{1-g^2}e^{\delta/2}\right) - \sin\,h^{-1}\left(\sqrt{1-g^2}e^{-\delta/2}\right)\right] + O\left(\frac{1}{\beta^2}\right). \end{aligned}\right\} \tag{A 8}$$

Over the final range we split the integrand into two parts. The first part is

$$I_{3a} = \int_{g(1+\delta/\beta)}^1 \frac{\mathrm{d}h}{\sqrt{1-h^2}} = \cos^{-1}[g(1+\delta/\beta)]. \tag{A 9}$$

The second part comes from substituting $h=g(1+x/\beta)$

$$\frac{1}{\sqrt{1-h^2+(g/h)^{\beta}-g^{\beta}}} - \frac{1}{\sqrt{1-h^2}} = \frac{g}{\beta}\left[\frac{1}{\sqrt{1-g^2+e^{-x}}} - \frac{1}{\sqrt{1-g^2}}\right] + O\left(\frac{1}{\beta^2}\right),$$

$$\begin{aligned} I_{3b} &= \int_{\delta}^1 \frac{g}{\beta}\left[\frac{1}{\sqrt{1-g^2+e^{-x}}} - \frac{1}{\sqrt{1-g^2}}\right] \\ &= \frac{2g}{\beta\sqrt{1-g^2}}\left[\sin\,h^{-1}\left(\sqrt{1-g^2}e^{\beta(1-g)/(2g)}\right)\right. \\ &\quad \left. -\sin\,h^{-1}\left(\sqrt{1-g^2}e^{\delta/2}\right) + \delta/2 - \frac{\beta(1-g)}{2g}\right] \\ &= \frac{2g}{\beta\sqrt{1-g^2}}\left[\log(2\sqrt{1-g^2}) - \sin\,h^{-1}\left(\sqrt{1-g^2}e^{\delta/2}\right) + \delta/2\right] + O\left(\frac{1}{\beta^2}\right). \end{aligned}$$

Adding these terms together, all the terms containing δ cancel (as they must) and we get

$$I = I_1 + I_2 + I_{3a} + I_{3b} = \cos^{-1}g + \frac{\log\left(2g\sqrt{1-g^2}\right)}{\beta\sqrt{1-g^2}} + O\left(\frac{1}{\beta^2}\right). \tag{A 10}$$

Taking only the leading order term, which does not depend on β we then have $b=g^{\beta}=\cos^{\beta}\phi$. The same analysis for $h(\theta)$ can be used to show

$$h(\theta) = \cos\theta \quad \theta < \phi. \tag{A 11}$$

For θ close to ϕ there is a boundary layer where $h\to 0$.

(*c*) $\alpha = 1$

When $\alpha=1$ equation (2.10) can be integrated once to give

$$ff_{\theta\theta} + f^2 + A = 0, \tag{A 12}$$

which can be written

$$\frac{f}{f_\theta}\frac{\mathrm{d}}{\mathrm{d}f}[f_\theta^2 + f^2 + 2A\log f] = 0, \tag{A 13}$$

and then integrated to give

$$f_\theta^2 = B - f^2 - 2A\log f. \tag{A 14}$$

For $\alpha=1$ and $g=h$ the normalization condition gives $B=1$ $A=b$. This can then be written as

$$\int_h^1 \frac{\mathrm{d}h}{\sqrt{1-h^2-2b\log h}} = |\theta|. \tag{A 15}$$

The leading contribution comes from $h\approx 1$ so we expand $\log h=(h-1)-(h-1)^2/2+O[(h-1)^3]$, which is absolutely convergent for $h>0$, $h<2$, to give

$$\int_h^1 \frac{\mathrm{d}h}{\sqrt{1-h}\sqrt{1+3b-h(1-b)}} = |\theta|. \tag{A 16}$$

The nature of this integral changes between trigonometric and hyperbolic depending on the sign of $1-b$, but both cases are equivalent since $\cos i\theta=\cos h\theta$, so we assume $b<1$. This then integrates to

$$\frac{\cos^{-1}[(h(1-b)+2b/1+b)]}{\sqrt{1-b}} = |\theta|, \tag{A 17}$$

thus

$$h(\theta) = \frac{(1+b)\cos(\theta\sqrt{1-b})-2b}{1-b}, \tag{A 18}$$

where b is the solution of the transcendental equation

$$2b = (1+b)\cos(\phi\sqrt{1-b}). \tag{A 19}$$

This solution is accurate to a few percent except for very small ϕ and θ. The accuracy could be improved by splitting the range of integration and making a different approximation for $-\log h \gg h^2$.

(d) $\alpha = 3/2$

When $\alpha = 3/2$, equation (2.16) results in the elliptic integral

$$|\theta| = \int_h^1 \frac{\sqrt{h}\mathrm{d}h}{\sqrt{(1-h)(b+h+h^2)}}. \tag{A 20}$$

There are four branch points at 0, 1, $-1/\delta$ and $-b\delta$, where $\delta = (1+\sqrt{1-4b})/(2b)$ so that $(b+h+h^2) = (1+\delta h)(b+h/\delta)$. For real and positive b all the branch points apart from $h=1$ have non-positive real part so we take a branch cut $[1, \infty]$ and restrict the integral to non-negative real part.

Changing variables to $x = \sqrt{h(1+\delta)/(1+\delta h)}$ and defining $m = \sqrt{b\delta^2 - 1}/\sqrt{b\delta(1+\delta)}$ and $\beta = \delta/(1+\delta)$ gives

$$\left.\begin{aligned}\theta &= \int_x^1 \frac{2x^2\mathrm{d}x}{\sqrt{b}(1+\delta)^{3/2}(1-\beta x^2)\sqrt{1-x^2}\sqrt{1-m^2x^2}} \\ &= \int_x^1 \frac{2\mathrm{d}x}{\delta\sqrt{b}\sqrt{1+\delta}\sqrt{1-x^2}\sqrt{1-m^2x^2}}\left[\frac{1}{1-\beta x^2} - 1\right] \\ &= \frac{2}{\delta\sqrt{b}\sqrt{1+\delta}}[\Pi(1,\beta,m) - F(1,m) - \Pi(x,\beta,m) + F(x,m)].\end{aligned}\right\} \tag{A 21}$$

F and Π are incomplete elliptic integrals of the first kind and third kind (Gradshteyn & Ryzhik 1980). The main result we need in this paper is that for $\phi = \pi/6$ $b \approx 7.65$ (by numerical solution). There appears to be no simple, explicit form for $h(\theta)$.

For small values of ϕ, b is large and one can use an asymptotic series in b as an approximation to get the solution

$$\theta = \left[\tfrac{1}{2}\cos^{-1}(2h-1) + \sqrt{h(1-h)}\right] b^{-(1/2)} + O(b^{-(3/2)}). \tag{A 22}$$

Thus $b \approx [\pi/(2\phi)]^2$.

(e) $\phi \ll 1$

For small wedge angles ϕ, b must be large and we can approximate as follows. $(1-h^2)/(h^{2-2\alpha}-1)$ is increasing for all $\beta > 0$ and attains its maximum value, on the range of integration, of $1/(\alpha-1)$ when $h=1$. Provided then that $b(\alpha-1) > 1$ we can expand the integrand and integrate term by term. Thus

$$\int_h^1 \frac{\mathrm{d}h}{\sqrt{1-h^2+bh^{2(1-\alpha)}-b}} = \int_h^1 \mathrm{d}h\left[\frac{1}{\sqrt{b}\sqrt{h^{2(1-\alpha)}-1}} + O(b^{-(3/2)})\right] \tag{A 23}$$

After a change of variables $x=h^{2(\alpha-1)}$, this is an incomplete elliptic integral equal to

$$\frac{B\left(\frac{\alpha}{2(\alpha-1)},\frac{1}{2}\right)-B_{h^{2(\alpha-1)}}\left(\frac{\alpha}{2(\alpha-1)},\frac{1}{2}\right)}{2(\alpha-1)\sqrt{b}}. \tag{A 24}$$

Thus

$$b=\frac{\beta^2 B\left(\frac{\alpha}{2(\alpha-1)},\frac{1}{2}\right)}{\phi^2}+O(1) \tag{A 25}$$

Using the normalized incomplete Beta functions $I_x(p,\ q)=B_x(p,\ q)/B(p,q)$ (Gradshteyn & Ryzhik 1980), and substituting in for b, the solution is then given implicitly by

$$I_{h^{2(\alpha-1)}}\left(\frac{\alpha}{2(\alpha-1)},\frac{1}{2}\right)=1-\theta/\phi. \tag{A 26}$$

References

Benjamin, T. B. 1968 Gravity currents and related phenomena. *J. Fluid Mech.* **31**, 209–248.

Bonnecaze, R. T. & Lister, R. 1999 Particle-driven gravity currents down planar slopes. *J. Fluid Mech.* **390**, 75–91.

Goldenfeld, N. 1992 *Lectures on phases transitions and the renormalization group*. Reading, MA: Addison-Wesley.

Gradshteyn, I. S. & Ryzhik, I. M. 1980 *Table of integrals, series and products*, 4th edn. New York: Academic Press.

McElwaine, J. N. & Nishimura, K. 2001 Ping-pong ball avalanche experiments. *Ann. Glaciol.* **32**, 241–250.

Simpson, J. E. 1997 *Gravity currents in the environment and the laboratory*. Cambridge: Cambridge University Press.

von Kármán, T. 1940 The engineer grapples with nonlinear problems. *Bull. Am. Math. Soc.* **46**, 615–683.

Webber, D.M, Jones, S. J. & Martin, D. 1993 A model of the motion of a heavy gas cloud released on a uniform slope. *J. Hazard. Mater.* **33**, 101–122.